All Sciences Proceedings

1st International Conference on Trends in Advanced Research

March 4-7, 2023 : Konya, Turkey

All Sciences Proceedings
http://as-proceeding.com/

ICTAR

Investigation of Thermodynamic Exhaust Line Losses of Hermetic Piston Compressor by FSI Method

Aykut Bacak* and Ali Pınarbaşı

Department of Mechanical Engineering, Faculty of Mechanical Engineering, Yildiz Technical University, 34349, Istanbul

(aykut.bacak@std.yildiz.edu.tr) Email of the corresponding author

Abstract – In the past few years, energy efficiency has become more critical because of the rise in the number of devices used in homes, the increase in the price of energy units, and the difficulty of getting energy. In addition to these worries, the laws passed about how energy is used in home appliances have made energy efficiency an essential factor in these devices. Hermetic reciprocating compressors are the heart of the refrigerator. They provide the circulation needed for the cooling process and use the most electricity in home refrigerators. Because of the compressor's importance, it is imperative to make it work better. This study used the fluid-solid interaction (FSI) method and CONVERGE CFD software to look at the thermodynamic performance of the hermetic reciprocating compressor, including the movement of the reed valves. The thermal performance of a refrigerator compressor using R600a under ASHRAE (54.4°C/-23.3°C) operating conditions was measured numerically and compared to the experimental results. Under ASHRAE operating conditions, the compressor's compression work converged by 2.1%, 1.79.%, and 5.4% for 1300, 2100, and 3000 RPM, while the cooling capacity converged by 3.0%, 1.28.%, and 2.12.%, respectively. In the investigation, the suction, discharge, and cylinder pressures and the displacements of the suction and discharge reed valves were compared to data from experiments.

Keywords – Include at least five keywords or phrases: Hermetic reciprocating compressor, FSI, reed valve, beam modeling

I. INTRODUCTION

Hermetic compressors are machines that move refrigerant through the cycle of systems like home air conditioners and refrigerators. The evaporation pressure and the superheated vapor temperature of the refrigerant are both examples of devices that are compressed by reducing their size until the condensing pressure is reached. Since hermetic reciprocating compressors are powered by an electric motor and compress and expand the refrigerant by moving the piston back and forth in the cylinder, it is expected that the amount of power needed to do the compression work will be low. In this study, the compression force of the piston in the cylinder and over the refrigerant is looked into. Because of this, the electric motor and its electrical efficiency are not taken into account. Instead, the topic is only brought up in relation to the thermo-fluid. So, the study talks about the thermodynamic discharge line of the hermetic reciprocating compressor (HRC) that was looked at. HRCs have been studied a lot from mechanical, thermo-fluid, and electrical points of view, and studies to improve their efficiency are still going on. Because of the energy crisis we are in, every bit of energy is now important. In the literature, both experimental and numerical methods have been used to study how to make HRCs use less energy. Here is a summary of what has been found:

Lee et al. [1] looked at how the discharge valve worked in both the rigid body model and the FSI model. Experiment data were used to compare each valve model and learn more about them. Only the valve lift of the FSI model was in line with the test. During the expansion phase of the compressor, backflow happens, and the 3D rigid body valve model couldn't predict this. On the other hand, the

3D FSI valve model could predict different displacement changes. The FSI model was the most accurate at figuring out the cooling capacity or EER of the linear compressor with a circular plate discharge valve.

Jia et al. [2] showed that a three-dimensional (3D) computational fluid dynamics (CFD) model could be used to solve both the transient flow inside a double-acting reciprocating compressor and the interaction between valve motion and pressure pulsation at the same time. Also, the effects of the Re-Normalisation Group (RNG) k- and Detached Eddy Simulation (DES) turbulence models on pressure pulsation were studied. Even though the valve lift is slightly different, a comparison of numerical models and real-world results showed that both turbulence models could accurately predict the thermodynamic performance. FFT analysis showed that the RNG k-e model was a good fit for the pressure pulsation below 500 Hz. At 420 rpm, the DES model could resolve frequencies above 1500 Hz with a 10% error range at much higher frequencies.

Yu et al. [3] used a three-dimensional fluid-structure interaction (FSI) model to predict the dynamic behavior of a reed valve in a 4800-rpm rotary compressor. The FSI model was proven correct by cylinder P-V graphs. FSI looked into how the reed hits the retainer and seat, how much stress it causes, and how fast it moves. For valve problems at 2.92, 5.39, and 13.54 m/s, the impact stress was 100.6, 124.9, and 148.4 MPa. The speed of an impact affects stress. When point one hits the valves, it speeds up from 7.95 m/s to 13.54 m/s. When point two hits the retainer, it bounces back at 6 m/s. At 345.95°, Reed is located. The impact speed of the retainer is faster than 2m/s. Impact stress stays high (133.2 MPa) because the reed hits the thin sealing band on the seat.

Peng et al. [4] used a 3D FSI model to simulate the whole compression cycle of a refrigeration compressor. Experiments were used to prove that the FSI model's thermodynamic compression analysis was correct. The FSI model looked at how the speed of the compressor's rotation and the parameters of the valve affected oscillation and the time it took for the valve to close. A reed valve is defined by the speed of its rotation that lets the most backflow and delayed closure happen. Simulations led to an empirical correlation that can be used to predict the normal speed of rotation. Backflow past the valve slowed the compressor's flow by a lot. At the average rate of 3200 r/min, which is the maximum backflow through the suction valve, volumetric efficiency drops by 7%. The backflow caused by the valve taking too long to close had a big effect on how well the compressor worked.

Wu et al. [5] made a 3D FSI model that was tested with the ADINA program to see how the piston-mounted valve moved as it oscillated. It was found that the valve on the piston has a lift integral that is 4.5 percent less than the valve on the cylinder head. The impact speed on the valve seat of the piston was less than that of the valve on the cylinder head. This showed that the suction valve mounted on the piston was more reliable. When it was seen that the lift of the valve was more than 0.1 mm, the valve opened. During the suction process, the crankshaft angle was 35,3° when the cylinder head valve was open and 200° when it was closed. When the piston valve was open, the crankshaft was at an angle of 34.7°. When the valve was closed, it was at an angle of 195°. Putting the reed valve on the piston did not make a big difference in how long it took for the reed valve to open.

He and his colleagues [6] used a 3D FSI refrigerator compressor model and results from experiments to figure out what the main reason was for the difference in performance. A pressure sensor was added after the pV indication diagram was made with a refrigerator compressor. The FSI model found that the operating conditions, rotation speed, and refrigerant all affect the change in cylinder pressure, which affects the performance of the compressor. The FSI model and output may help test and improve the performance of compressors. According to the power compression calculation method, 209.67W and 184.36W of the total compression effort come from the numerical integral experiment and simulation, respectively. Because its polytropic exponent is 1.0944, R600a shrinks and grows like R134a. The polytropic exponent of CO2 is 1.2602, which is more important than those of R600a and R134a. CO2 is more useful than either R600a or R134a.

Bacak et al. [7] studied the oscillation motion of the suction and discharge reed valves, compression power, and mass flow rate of an HRC operating under ASHRAE (54.4°C/-23.3°C) at the speed of 2100 rpm and other specific refrigerator operating conditions such as (25°C/-20°C) and (40°C/-25°C) at the speeds of 1300 and 1600 rpm. When

experimental data and numerical outputs from the RNG k- turbulence model are looked at, it is shown that the turbulence model is reliable for predicting thermodynamic performance and valve lift. Under ASHRAE and different operating conditions, the difference between experimental and numerical results for compression power is 1.7%, -0.6%, and 3.44 %, and the difference for mass flow rate is 1.28 %, 0.6 %, and 2.44 %.

Yu et al. [8] suggested a three-dimensional FSI model for how the discharge valve of a rotary compressor moves. Experiments with the pressure in the compression chamber showed that the FSI model could accurately predict how a dynamic valve would behave. Another FSI model with an open discharge port and a more simple cylinder shape shows that the valve model can't ignore the fact that the cylinder and roller cover part of the discharge port. This simplified FSI model has a flow energy loss of 68.8% through the discharge valve and a valve reed impact velocity on the retainer that is 2.9 m/s faster. The valve reed is at an angle because the cylinder covers part of the port for releasing air.

Hopfgartner et al. [9] looked at a suction valve that closes not with preload but with an electromagnetic coil in the neck of the suction muffler. Before the piston hits the bottom dead center (BDC), voltage is sent to the coil, which creates a magnetic force. The modified valve and the electromagnetic wave are studied using numerical models of FSI of HRC reed valves and calorimeter test bench trials. Calculations show that the ASHRAE cycle (-23 °C/55 °C) cut electricity use by 0.68 percent. The total mass-flow rate goes down by 0.3 percent because the suction port mass-flow rate goes up from 0.26 to 1.6%. The simulation's prediction that power consumption would go down by 0.71 percent, cooling capacity would go down by 0.32 percent, and COP would go up by 0.39 percent was confirmed by measurements. The COP is 1.72 percent higher for a second operating state.

Rowinski and Davis [10] used a Cartesian cut-cell finite volume to model an HRC. The cut-cell method represents discrete cell volumes correctly without the need to match the border geometry to a grid. At each time step, local flow variable gradients change the grid based on where the immediate boundaries are. Running at larger time steps has no effect on the suction process, but the discharge process is more sensitive. At CFL 4.0, a 2 percent change in maximum pressure is caused by running at larger time steps. CFL numbers exceeding 50 percent degrade runtime. CFL of 4.0 shortens the time it takes to run the program because each transport equation must be solved to the set tolerance. Modeling how valve seats touch affects numbers. 1E-4, 1E-5, and 1E-6-m gaps were studied. 1E-5 m worked. If the gap was too small, the time step was very limited, and if it was too big, the flow zones were a little too big.

Almbauer et al. [11] used a simulation of an HRC to compare the assumption of an ideal gas with a real gas approach. Also, the results are compared to the data from the experiments, and the differences are found. All simulations have been done by making valves look like flat plates that move in parallel. The results show that there aren't many differences between the ideal gas equation of state and how gases really act. For industrial applications, especially, the benefit of significantly shorter computation times is more important than the small improvement in accuracy. Also, using real gas models tends to make simulations less stable, which can lead to results that do not converge. In conclusion, it can be said that using the right boundary conditions for the walls of the cylinder and the suction and discharge lines is much more important than using an enhanced gas model.

Rowinski et al. [12] used an automated meshing numerical grid to model an HRC (AMR). At each time step, the grid is changed by the local flow field variables. This grid, which is made up of cut cells, fits the volume of the fluid and lets all the boundary surfaces move. Reed valves that change shape work with flow through a clear two-way linkage. Fluids are solved with finite-volume methods, while solids are solved with finite-element models. Measure the mass flow rate, pressure, temperature, and valve lift for two operating conditions and R-404a and R-449a working fluids to make sure the model is correct. The height of clearance was raised to 0.1 mm. Second, cylinder bore-piston crevice leakage is shown by an orifice flow equation. Check out these two changes, which could cause predicted flow rates to drop by 10–20%. During the opening of the discharge valve, the pressure traces that were seen and those that were simulated are similar. For all four operating sites, the model consistently underestimates the size by 2–5 percent, and it correctly predicts the frequency of cylinder expansion pressure waves.

Dhar et al. [13] created the method for making and simulating single-piston compressor models. The model and simulation used real gas fluid properties and geometry. The fully coupled 3-D transient CFD simulation of a piston compressor and a flip valve is fast and gives real results. Before the suction stroke, the outlet valve opens about 30° and then closes before the suction stroke. During the suction stroke, 40° after the top dead center of the crank, the valve opens (TDC). During suction, the suction valve moves back and forth and closes 30° into compression. Because of the retainer, the opening of the discharge valve is smaller than that of the suction valve, and it closes more quickly. Because it is less rigid, the suction valve moves and opens slowly.

II. NUMERICAL METHOD

Most people know that a connection between the flow of refrigerant and the movement of the reed valve is what makes a refrigerator compressor work. A pressure difference will also change the flow field of the refrigerant because the reed valve will be bent out of shape. Because of this, it is hard to imitate how refrigerator compressors work as a whole because not only must the governing equations of structure and fluid be solved, but the interaction between the two must also be taken into account. This makes it hard to make the exact same conditions that the compressors work in. In this article, we use a commercial program called CONVERGE version 3.0 to make a 3D FSI model that can be used to study how compressors work. As part of this FSI research, the compressor model is split into a fluid domain and a structural domain so that each can be studied separately.

The compressor concept is based on the idea that the motion of a continuous domain of refrigerant fluid is subject to the same rules of classical mechanics and thermodynamics as any other system. As demonstrated by the equations, they are also expressible in conservative forms of mass, momentum, and energy. (1)–(4).

Continuity equation:

$$\frac{\partial \rho}{\partial t} + \nabla\left(\rho \vec{V}\right) = 0 \tag{1}$$

Momentum equation:

$$\rho\left(\frac{\partial \vec{V}}{\partial t} + \left(\nabla \vec{V}\vec{V}\right)\right) = -\nabla p + \nabla \tau \tag{2}$$

The stress tensor is given by:

$$\tau = \mu\left[\nabla \vec{V} + \left(\nabla \vec{V}\right)^{T}\right] - \frac{2}{3}\vec{V}I \tag{3}$$

Energy equation:

$$\frac{\partial}{\partial t}\left[\rho\left(E + \frac{1}{2}V^{2}\right)\right] + \nabla.\left[\rho V\left(E + \frac{1}{2}V^{2}\right)\right] = \nabla.(k\nabla T) + \nabla.(-pV + \tau.V) + Q \tag{4}$$

where ρ is the density, t is the time, V is the velocity vector, τ is the stress tensor of the fluid, E is the total internal energy, k is the thermal conductivity of the fluid, T is the thermodynamic temperature, Q is the specific rate of heat generation.

Using the Redlich–Kwong model, R600A is thought to have a low-pressure, low-speed compressible flow. The RNG k- turbulence model is used to simulate turbulent flow in the fluid domain. The standard pressure interpolation method is used, and the PISO method is used to solve the problem of pressure and velocity being tied together. Here is a list of the transport equations for turbulence energy and the rate of dissipation [14]:

$$\frac{\partial}{\partial t}(\rho k) + \frac{\partial}{\partial x_i}(\rho k u_i) = \frac{\partial}{\partial x_j}\left[\left(\mu + \frac{\mu_t}{\sigma_k}\right)\frac{\partial k}{\partial x_j}\right] + P_k - \rho\varepsilon \tag{5}$$

$$\frac{\partial}{\partial t}(\rho \varepsilon) + \frac{\partial}{\partial x_i}(\rho \varepsilon u_i) = \frac{\partial}{\partial x_j}\left[\left(\mu + \frac{\mu_\varepsilon}{\sigma_\varepsilon}\right)\frac{\partial \varepsilon}{\partial x_j}\right] + C_{1\varepsilon}\frac{\varepsilon}{k}P_k - C_{2\varepsilon}^{*}\rho\frac{\varepsilon^2}{k} \tag{6}$$

$$C_{2\varepsilon}^{*} = C_{2\varepsilon} + \frac{C_\mu \eta^3\left(1 - \frac{\eta}{\eta_0}\right)}{1 + \beta\eta^3} \tag{7}$$

$$\eta = \frac{Sk}{\varepsilon} \tag{8}$$

$$S = \sqrt{\left(2S_{ij}S_{ij}\right)} \quad (9)$$

where μt is the turbulent viscosity. Cμ, σk, σε, Cε1, Cε2, η0 and β are the model constants. Blending the relevant constants from the conventional k-ε model is used to get these values. The following values are the two models' constants: Cμ = 0.0845, σk = 0.7194, σε = 0.7194, Cε1 = 1.42, Cε2 = 1.68, η0 = 4.38, β = 0.012.

The finite-volume method may solve the continuity, momentum, and energy equations. In the middle of each computational cell, all the model values are put together. Using a method proposed by Rhie and Chow [15], it is possible to keep the speed and pressure fields from crossing each other. This question is answered with a variable time step that starts at 1E-07 seconds, has a minimum of 1E-08 seconds, and a maximum of 2E-06 seconds. The time step has been set up for CFLs with a wattage between 1 and 5. A method based on variable time steps is used to keep the system stable and, if possible, speed up the time step. Courant-Friedrichs-Lewy (CFL) parameters, which define the time step, are affected by the size and speed of local cells, the speed of sound, and the way things spread out. There are FSI events for both rigid bodies and beams that bend. These abilities are like what open and closed events can do. As an alternative to times, rigid or beam FSI events may be defined in terms of translation lengths or degrees of rotation. In arguments, FSI events go beyond what would typically happen. Open events turn off separate triangles to make it easier to move between certain places. After an event that closes a zone, disconnection triangles make it impossible to move between zones. Triangles that don't connect set off symmetry border conditions. Changes to the time step don't help CONVERGE line-up events with time steps. In conclusion, CONVERGE runs each time step's events. After an event, the time step is cut by ten to show how shocked the domain is by closing or joining parts.

Message Passing Interface (MPI) is used for all parallel simulations, and the nontrivial automated domain decomposition technique of Karypis [16] is used to control how the load is spread out. If the computational volume changes or Adaptive Mesh Refinement is used to add cells, the cells may not be evenly spread out (AMR). Senecal et al. [17] came up with the Cartesian cut-cell method that is used in this research. The model starts with a triangulated surface that shows the volume of the numerical volume and is filled with the orthogonal basis grid size chosen by the user. Where the triangulated surface overlaps the base grid, the base grid cells are split into polyhedral shapes with arbitrary lengths of sides. No matter how big the base grid is, the volume of the cut cells will be the same as the volume of the triangulated surface. Because mesh generation is automated, even the most complicated boundary shapes and movements can be made with little help from a person. This method is easy to compute and has strong numerical stability because it uses regular orthogonal grids. The finite-volume method is used to solve these conservation equations because it is the best way to do it. By the time we get to the middle of the number cells, we already have all of the model values.

III. RESULTS AND DISCUSSION

The exhaust line thermodynamic losses for the hermetic reciprocating compressor's speed of 1300 and 2100 rpm examined in Figure 4.108 are shown depending on the exhaust valve leaf thickness and valve length. When the thermodynamic exhaust line losses of the hermetic reciprocating compressor examined for a compressor speed of 1300 rpm and a limit height of 0.8 mm are concerned, it is determined that by increasing the valve leaf length from 14,722 mm to 16,222 mm, the thermodynamic exhaust line losses increase between 0.39% and 6.54%, while the leaf length is 17.722 mm. With the extension to the length, it has been determined that these losses change in the form of a maximum increase of 1.11% and a decrease of 16.43%. It has been observed that the thermodynamic exhaust line losses increase with the increase of the exhaust valve leaf thickness. Ranges of exhaust line thermodynamic losses due to thickness increase for exhaust valve leaf lengths of 14,722, 16,222 and 17,722 mm 37%, 39% and 13%, respectively.

When the thermodynamic exhaust line losses of the hermetic reciprocating compressor examined for

a compressor speed of 1300 rpm and a limit height of 1.05 mm are examined, it was determined that the thermodynamic exhaust line losses increased between 7.39% and 9.21% by increasing the valve leaf length from 14,722 mm to 16,222 mm, while the leaf length was 17,722 mm. With the extension to the length, it has been determined that these losses change in the form of a maximum increase of 7.85% and a decrease of 1.59%. It has been observed that the thermodynamic exhaust line losses increase with the increase of the exhaust valve leaf thickness. Ranges of exhaust line thermodynamic losses due to thickness increase for exhaust valve leaf lengths of 14,722, 16,222 and 17,722 mm 32%, 32% and 20%, respectively.

When the thermodynamic exhaust line losses of the hermetic reciprocating compressor examined for a compressor speed of 1300 rpm and a limit height of 1.25 mm are examined, it is determined that by increasing the valve leaf length from 14,722 mm to 16,222 mm, the thermodynamic exhaust line losses increase between 2.94% and 7.7%, while the leaf length is 17.722 mm. With the extension to the length, it has been determined that these losses change in the form of a maximum increase of 20.18% and a decrease of 3.87%. It has been observed that the thermodynamic exhaust line losses increase with the increase of the exhaust valve leaf thickness. For 14,722, 16,222 and 17,722 mm exhaust valve leaf lengths, the orders of exhaust line thermodynamic losses due to thickness increase are 38%, 24% and 25%, respectively.

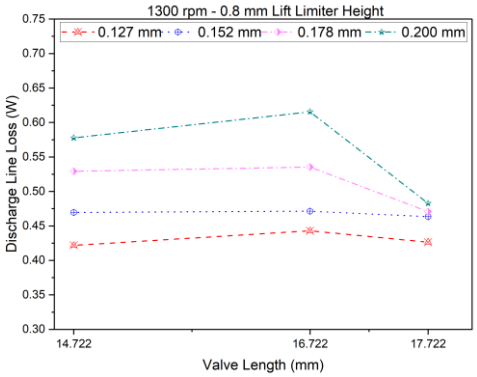

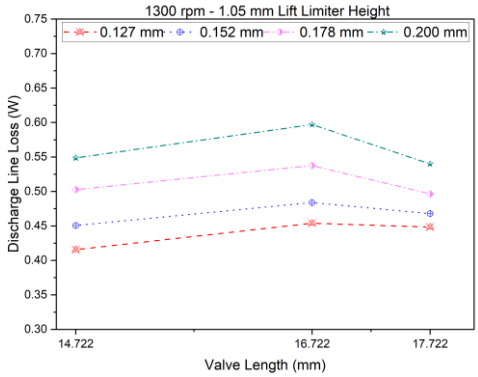

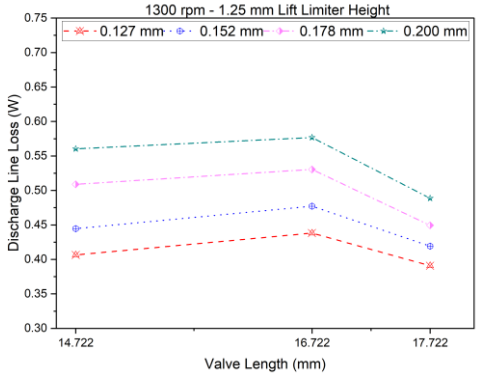

When the thermodynamic exhaust line losses of the hermetic reciprocating compressor examined for a compressor speed of 2100 rpm and a limit height of 0.8 mm are examined, it is determined that the thermodynamic exhaust line losses increase between 2.30% and 13.66% by increasing the valve leaf length from 14,722 mm to 16,222 mm, while the leaf length is 17,722 mm. It has been determined that these losses change in the form of a maximum increase of 9.15% and a decrease of 7.54% with the extension to the length. It has been observed that the thermodynamic exhaust line losses increase with the increase of the exhaust valve leaf thickness. Ranges of exhaust line thermodynamic losses due to thickness increase for exhaust valve leaf lengths of 14,722, 16,222 and 17,722 mm 31%, 18% and 11%, respectively.

When the thermodynamic exhaust line losses of the hermetic reciprocating compressor examined for a compressor speed of 2100 rpm and a limit height of 1.05 mm are examined, it is determined that by increasing the valve leaf length from 14,722 mm to 16,222 mm, the thermodynamic exhaust line losses increase in the range of 5.66% to 11.42 mm, while the leaf length is 17.722 mm. With the extension to

the length, it has been determined that these losses change in the form of a maximum increase of 4.28% and a decrease of 4.51%. It has been observed that the thermodynamic exhaust line losses increase with the increase of the exhaust valve leaf thickness. Ranges of exhaust line thermodynamic losses due to thickness increase for exhaust valve leaf lengths of 14,722, 16,222 and 17,722 mm 23%, 29% and 14%, respectively.

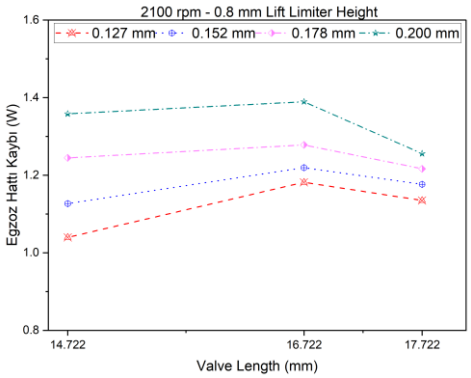

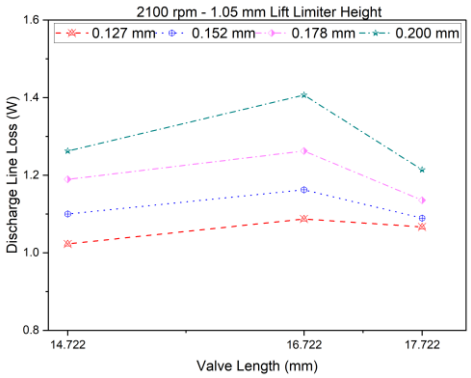

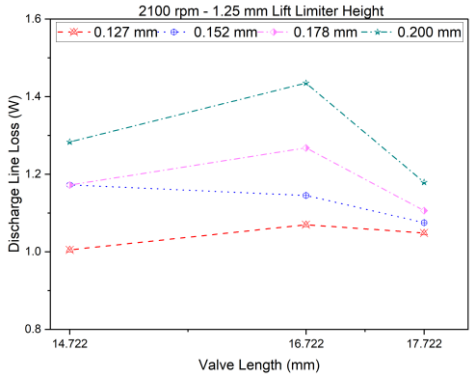

The exhaust line thermodynamic losses for the 3000 rpm compressor speed of the hermetic reciprocating compressor examined in Figure 4.109 are shown depending on the exhaust valve leaf thickness and valve length.

When the thermodynamic exhaust line losses of the hermetic reciprocating compressor examined for 3000 rpm compressor speed and 0.8 mm restriction height are examined, it is determined that by increasing the valve leaf length from 14,722 mm to 16,222 mm, the thermodynamic exhaust line losses increase between 9.33% and 15.37%, while the leaf length is 17.722 mm. It has been determined that these losses increase by a maximum of 6.99% and 10.21% with the extension to the length. It has been observed that the thermodynamic exhaust line losses increase with the increase of the exhaust valve leaf thickness. The orders of exhaust line thermodynamic losses due to thickness increase for exhaust valve leaf lengths of 14,722, 16,222 and 17,722 mm, respectively.

16%, 10% and 14%.

When the thermodynamic exhaust line losses of the hermetic reciprocating compressor examined for 3000 rpm compressor speed and 1.05 mm restriction height are examined, it is determined that by increasing the valve leaf length from 14,722 mm to 16,222 mm, the thermodynamic exhaust line losses increase in the range of 3.24% to 10.61%, while the leaf length is 17,722 mm. It has been determined that these losses change in the form of a maximum increase of 0.82% and a decrease of 6% with the extension to the length. It has been observed that the thermodynamic exhaust line losses increase with the increase of the exhaust valve leaf thickness. Exhaust valve leaf lengths of 14,722, 16,222 and 17,722 mm

The orders of exhaust line thermodynamic losses due to the increase in thickness are 16%, 24% and 8%, respectively.

When the thermodynamic exhaust line losses of the hermetic reciprocating compressor examined for 3000 rpm compressor speed and 1.25 mm restriction height are examined, it is determined that by increasing the valve leaf length from 14,722 mm to 16,222 mm, the thermodynamic exhaust line losses increase in the range of 6.91% to 10.33%, while the leaf length is 17.722 mm. It has been determined that these losses change in the form of a maximum increase of 0.38% to 4.76% with the extension to the length. It has been observed that the thermodynamic exhaust line losses increase with the increase of the exhaust valve leaf thickness. For 14,722 and 16,222 exhaust valve leaf lengths, the extent of exhaust line thermodynamic losses due to the increase in

thickness is 17%, while this value is 14% for 17,722 mm length.

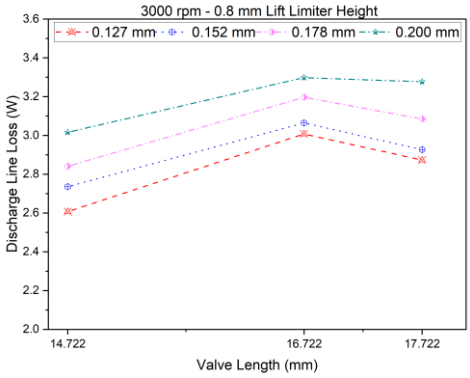

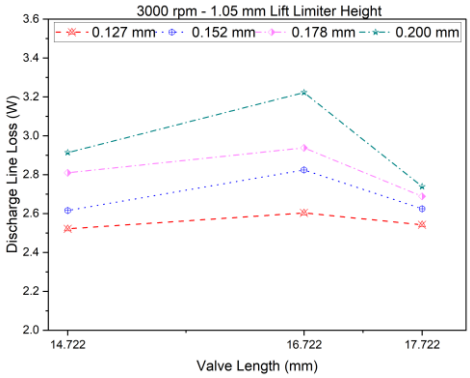

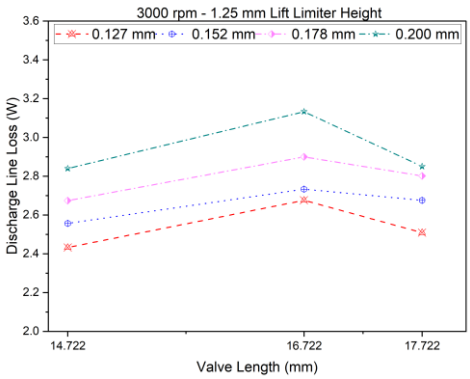

IV. CONCLUSION

The FSI method is suggested in this study as a way to study the thermodynamic process and the movement of the valves in the hermetic reciprocating compressor. On the basis of the suggested model, the design parameters for optimizing the compressor's discharge line and discharge port losses are found, and the results are shown below:

1. When the relationship between the exhaust line thermodynamic losses and the restriction height is examined, it has been determined that the low limit height will increase the losses since the velocity of the refrigerant and hence the gas forces will be high so that the mass in the cylinder can be discharged even if the exhaust valve leaf is fully open.
2. When the relationship of exhaust line losses with exhaust valve leaf thickness is examined, it will lead to an increase in losses and a decrease in relative efficiency, since the mass and inertia of the valve will increase with an increase in exhaust valve leaf thickness, requiring more work on the refrigerant, and since the refrigerant will be more dominant than the gas forces.

Acknowledgment

This research is based on the Yildiz Technical University doctoral dissertation. Convergent Science supplied licensing and technical support for CONVERGE for this project.

REFERENCES

[1] Hwang, I. S., Park, S. J., Oh, W., & Lee, Y. L. (2017). Linear compressor discharge valve behavior using a rigid body valve model and a FSI valve model. International Journal of refrigeration, 82, 509-519.

[2] Zhao, B., Jia, X., Sun, S., Wen, J., & Peng, X. (2018). FSI model of valve motion and pressure pulsation for investigating thermodynamic process and internal flow inside a reciprocating compressor. Applied Thermal Engineering, 131, 998-1007.

[3] Yu, X., Tan, Q., Ren, Y., Jia, X., & Jin, L. (2017). Numerical study of the reed valve impact in the rotary compressor by FSI model. Energy Procedia, 105, 4890-4897.

[4] Tao, W., Guo, Y., He, Z., & Peng, X. (2018). Investigation on the delayed closure of the suction valve in the refrigerator compressor by FSI modeling. International Journal of Refrigeration, 91, 111-121.

[5] Wu, W., Guo, T., Peng, C., Li, X., Li, X., Zhang, Z., ... & He, Z. (2022). FSI simulation of the suction valve on the piston for reciprocating compressors. International Journal of Refrigeration, 137, 14-21.

[6] He, Z., Jian, Z., Wang, T., Li, D., & Peng, X. (2017, August). Investigation on the variation of pressure in the cylinder of the refrigerator compressor based on FSI model. In IOP Conference Series: Materials Science and Engineering (Vol. 232, No. 1, p. 012005). IOP Publishing.

[7] Bacak, A., Pınarbaşı, A., & Dalkılıç, A. S. (2023). A 3-D FSI simulation for the performance prediction and valve dynamic analysis of a hermetic reciprocating compressor. International Journal of Refrigeration. Accepted paper.

[8] Tan, Q., Pan, S. L., Feng, Q. K., Yu, X. L., & Wang, Z. L. (2015). Fluid–structure interaction model of dynamic behavior of the discharge valve in a rotary compressor. Proceedings of the Institution of Mechanical Engineers, Part E: Journal of Process Mechanical Engineering, 229(4), 280-289.
[9] Hopfgartner, J., Posch, S., Zuber, B., Almbauer, R., Krischan, K., & Stangl, S. (2017, August). Reduction of the suction losses through reed valves in hermetic reciprocating compressors using a magnet coil. In IOP conference series: materials science and engineering (Vol. 232, No. 1, p. 012034). IOP Publishing.
[10] Rowinski, D. H., & Davis, K. E. (2016). Modeling reciprocating compressors using a Cartesian cut-cell method with automatic mesh generation.
[11] Lang, W., Almbauer, R., Berger, E., & Nagy, D. (2010). Comparative Study of Two Different Equations of State for Modelling a Reciprocating Compressor for the Refrigerant R600a.
[12] Rowinski, D. H., Sadique, J., Oliveira, S. J. D., & Real, M. (2018). Modeling A Reciprocating Compressor Using A Two-Way Coupled Fluid And Solid Solver With Automatic Grid Generation And Adaptive Mesh Refinement.
[13] Dhar, S., Ding, H., & Lacerda, J. (2016). A 3-D transient CFD model of a reciprocating piston compressor with dynamic port flip valves.
[14]Issa, R. I., 1986. Solution of the implicitly discretised fluid flow equations by operator-splitting. Journal of Computational Physics. 62(1), 40-65.
[15]Rhie, C. M., & Chow, W. L. (1983). Numerical study of the turbulent flow past an airfoil with trailing edge separation. AIAA journal, 21(11), 1525-1532.
[16]Karypis, G., 1998. A software package for partitioning unstructured graphs, partitioning meshes and computing fill-reducing orderings of sparse matrices.
[17]Senecal, P. K., Richards, K. J., Pomraning, E., Yang, T., Dai, M. Z., McDavid, R. M., ... & Shethaji, T. (2007). A new parallel cut-cell Cartesian CFD code for rapid grid generation applied to in-cylinder diesel engine simulations (No. 2007-01-0159). SAE Technical Paper.